Journal of Alloys and Compounds 509 (2011) L228–L231

Contents lists available at ScienceDirect

Journal of Alloys and Compounds

journal homepage: www.elsevier.com/locate/jallcom

Letter

Chloride-substitution in sodium borohydride

Jørn Eirik Olsen*, Magnus H. Sørby, Bjørn C. Hauback

Institute for Energy Technology, Physics Department, P.O. Box 40, NO-2027 Kjeller, Norway

ARTICLE INFO

Article history:
Received 28 February 2011
Received in revised form 29 March 2011
Accepted 30 March 2011
Available online 5 April 2011

Keywords:
Metal hydrides
Mechanochemical processing
Synchrotron radiation
Thermal analysis
Thermodynamic properties
X-ray diffraction

ABSTRACT

The changes in structure and stability of $NaBH_4$ on Cl-substitution obtained in mechanochemical reactions between $NaBH_4$ and NaCl have been investigated by conventional and synchrotron radiation powder X-ray diffraction, differential scanning calorimetry and temperature programmed desorption. Powder X-ray diffraction shows an apparent full homogeneity range between $NaBH_4$ and NaCl, giving $Na(BH_4)_{1-x}Cl_x$ phase where x corresponds to the ratios of the initial reagents. Differential scanning calorimetry indicates that the Cl-substitution stabilizes the product, by increasing temperature for melting and desorption.

1. Introduction

Lately there has been an increased focus on renewable energy sources as a replacement for the present use of fossil fuels. Many of these energy outputs are, however, not constant in time, and therefore there is huge interest in developing efficient, robust, rechargeable energy storage systems. Hydrogen is considered as an attractive energy carrier, as it is an abundant element with high energy density which can be generated from any energy sources and converted to energy in a fuel cell with a high efficiency and water as the only by-product. Effective storage of hydrogen is, however, a major bottleneck for its widespread use as an energy carrier. Ongoing research shows that metal borohydrides can store hydrogen in a safe and efficient way, with volumetric densities significantly exceeding those in compressed or liquid hydrogen, and high gravimetric hydrogen density, e.g. 18.6 wt% for $LiBH_4$ [1–5]. Most of the light metal borohydrides, e.g. $LiBH_4$, are thermodynamically too stable for storage applications. $Ca(BH_4)_2$ and $Mg(BH_4)_2$ has theoretically predicted thermodynamics which should give hydrogen release close to room temperature. However, the experimental hydrogen desorption temperatures are much higher, probably due to kinetic barriers [6–8], and furthermore the desorption process is very complicated [9]. Another well-studied material is $NaBH_4$ [5,6,10–13], with an attractive capacity of 10.8 wt% hydrogen, but the challenge is the high stability as $NaBH_4$ melts at 505 °C [10] and decompose after melting [10,13]. Moreover, rehydrogenation of the desorption products is not viable at reasonable conditions [5].

A possible route for changing the thermodynamic properties is by anion substitution. Brinks et al. [14] showed that substitution of hydrogen with fluorine in the complex hydride Na_3AlH_6 had a destabilizing effect. A phase $Na_3AlH_{6-x}F_x$ with $x \sim 4$, synthesized from NaF, Al, TiF_3 (3 mol%) and H_2, had a large increase in equilibrium pressure compared to Na_3AlH_6, changing the plateau pressure at 120 °C from 1.5 bar to about 25 bar. Eigen et al. [15] confirmed that fluorine substitution in Na_3AlH_6 has a destabilizing effect, and thus the reversible hydrogen storage abilities were improved.

Anion substitutions, where a portion of the BH_4^- groups is replaced by a halide anion (Cl^-, Br^- or I^-) have been reported to affect the physical properties of $LiBH_4$ [16–21]. Ball milling and annealing of $LiBH_4$ and LiCl led to a solid solution of $Li(BH_4)_{1-x}Cl_x$ [16], with up to $x = 0.30$ for o-$LiBH_4$ (orthorhombic, low-temperature phase) and up to $x = 0.42$ for h-$LiBH_4$ (hexagonal, high-temperature phase) [17]. Furthermore the temperature for the orthorhombic to hexagonal phase transition was significantly reduced and the electrical conductivity increased [18]. Orimo et al. [19–21] showed that solid solutions of $Li(BH_4)_{1-x}I_x$, with $0 < x < 0.8(\pm 0.2)$, decreases the structural phase transition temperature with increasing iodine-content. With $x = 0.20$ the phase transition temperature is decreased from 110 to 53 °C, and for $x > 0.33$ the h-$LiBH_4$ is stabilized at room temperature.

Composites of $Ca(BH_4)_2$ and 10 mol% CaX_2, $X = F^-$ or Cl^-, has been reported to have some effect on the dehydrogenation properties of $Ca(BH_4)_2$ [22]. The $CaCl_2$ completely dissolved into $Ca(BH_4)_2$ making a solid solution, while CaF_2 only resulted in a solid solution with the decomposition product CaH_2. Both composites changed

* Corresponding author. Tel.: +47 63806067.
E-mail address: jorn.eirik.olsen@ife.no (J.E. Olsen).

0925-8388/$ – see front matter © 2011 Elsevier B.V. All rights reserved.
doi:10.1016/j.jallcom.2011.03.166

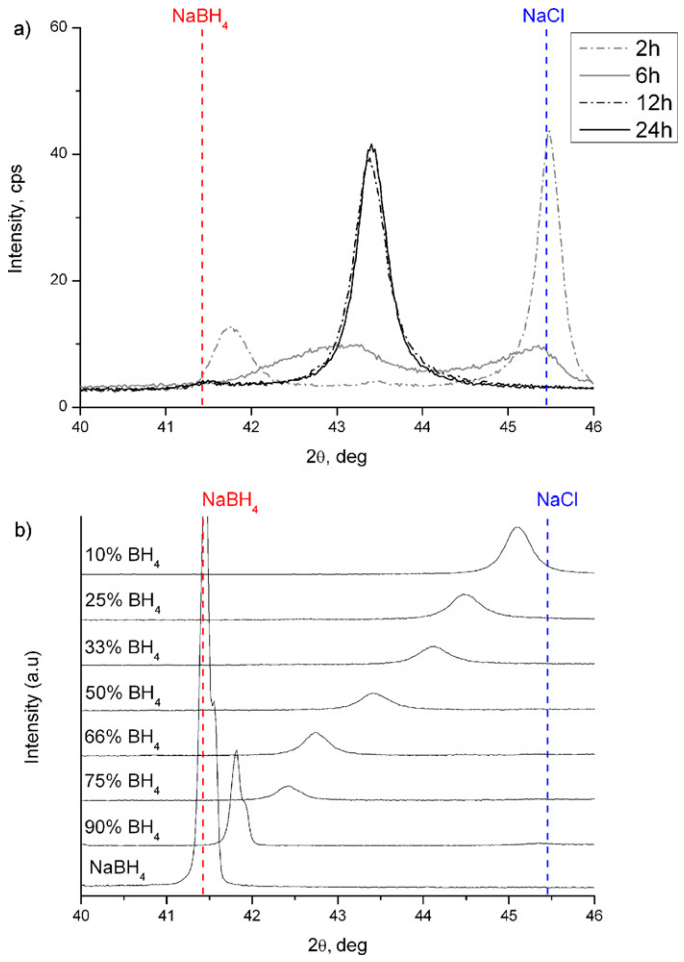

Fig. 1. (a) PXD patterns showing the 220 reflection from the 1:1 mixture of $NaBH_4$ and NaCl after different ball milling times. Grey dashed line is after 2 h, gray line is after 6 h, black dashed line is after 12 h and black line is after 24 h of ball milling. (b) PXD patterns (220 reflection) corresponding to the different compositions after 24 h of ball milling. The expected peak positions for pure $NaBH_4$ and NaCl are indicated by dashed vertical lines.

the decomposition pathway, but did not significantly affect the thermodynamics.

A recent study reports a considerable chloride-substitution in $NaBH_4$ after ball-milling with different transition metal chlorides [23], resulting in the formation of stable $Na(BH_4)_{1-x}Cl_x$ solid solution with x between 0.65 and 0.73.

In the present work, systematic syntheses of such phases have been performed from $NaBH_4$ and NaCl in different mixing ratios to determine the homogeneity range and the changes in thermodynamic properties with increasing substitution.

2. Experimental

Mixtures containing pure $NaBH_4$ (Sigma–Aldrich, ≥96%) and NaCl (ABCR, 99.999%) in the molar ratios 9:1, 3:1, 2:1, 1:1, 1:2, 1:3, 1:9 were milled in Ar atmosphere using a Fritsch Pulverisette 7 Planetary Mill. All samples were treated equally, with a ball-to-powder mass ratio of 18:1 and a milling speed of 500 rpm for 24 h. In addition samples were taken out after 2, 6 and 12 h of milling, respectively. Sample handling was carried out in MBraun Unilab glove boxes filled with purified Argon (<1 ppm O_2 and H_2O) to avoid contamination.

Powder X-ray diffraction (PXD) patterns were collected in transmission mode using Cu Kα radiation (λ = 1.5405 Å) in a Bruker AXS D8 Advance Diffractometer equipped with a Göbbel mirror and a LynxEye™ 1D strip detector. The diffraction patterns were obtained using rotating boron glass capillaries (0.8 mm ⌀) filled and sealed under Ar atmosphere. Pure Si was added as internal standard (ABCR, APS 1–5 μm, 99.999%). The measurements were done in the 2θ range = 20–60°, with Δ2θ = 0.02° and 2.7 s/step scanning rate.

Table 1
The refined unit cell parameters and composition for all the samples. Estimated standard deviations are given in parenthesis.

Sample ($NaBH_4$:NaCl)	Unit-cell parameter (a) (Å)	Composition (Vegard's law) $Na(BH_4)_{1-x}Cl_x$	Experimental data from instrument
9:1	6.1134(2)	0.10	Bruker AXS D8
3:1	6.0313(1)	0.25	SNBL, ESRF
2:1	5.9705(2)	0.37	Bruker AXS D8
1:1	5.8864(2)	0.53	Bruker AXS D8
1:2	5.7942(3)	0.71	Bruker AXS D8
1:3	5.7626(1)	0.77	SNBL, ESRF
1:9	5.6816(1)	0.92	Bruker AXS D8

High-resolution synchrotron radiation powder X-ray diffraction (SR-PXD) data were collected at the Swiss-Norwegian Beam Line (SNBL, BM01B) at ESRF, Grenoble, France. The instrument is equipped with 6 scintillation detectors mounted with 1.1° separation in 2θ, each with a secondary monochromator. The measurements were performed in the 2θ range = 7–35° with λ = 0.50123 Å, using rotating boron glass capillaries (0.5 mm ⌀) filled and sealed under Ar atmosphere. The data were combined with a 0.003° binning step size.

All PXD-data were analysed by the Rietveld method using the GSAS software package [24] with the EXPGUI [25] user interface.

Differential scanning calorimetry (DSC) measurements were performed using a Setaram Sensys DSC. The samples were put into high pressure stainless steel crucibles, and heated to 600 °C, with a heating rate of 2 °C/min.

In situ SR-PXD data were collected using a MAR345 image plate detector at the Swiss-Norwegian Beam Line (SNBL, BM01A) at ESRF, Grenoble, France. The data were measured at a sample-to-detector distance of 250 mm, with λ = 0.70947 Å. The samples were containing in single-crystal sapphire capillaries fixed in a Swagelok fitting and kept under dynamic vacuum. Exposure times of 30 s were used and 90 s were needed for read-out, thus giving a diffraction pattern every 2 min. The capillary was rotated 30° during exposure to improve the powder averaging. Measurements were carried out between room temperature and 600 °C using a hot air blower. The constant heating rate was 8 °C/min up to 400 °C and then 2 °C/min. Masking of the sapphire reflections and data integration was done using the Fit2D program [26]. Calibration was performed using a NIST LaB_6 standard.

Temperature programmed desorption (TPD) was performed under dynamic vacuum up to 600 °C using an in-house built setup. A 2 °C/min heating rate and approximately 50 mg of sample were used for all the measurements. The gas release was analysed with a MKS Microvision-IP Rest Gas Analyser (RGA).

3. Results and discussion

$NaBH_4$ and NaCl are isostructural with a NaCl-type structure and unit cell parameter a = 6.1635 Å and a = 5.6402 Å, respectively [27,28]. PXD patterns of a 1:1 sample of $NaBH_4$ and NaCl after 2, 6, 12 and 24 h of milling are shown in Fig. 1. After 2 h of milling, the unit cell parameter of $NaBH_4$ has decreased by 0.05 Å which is evident from the shift of positions of the Bragg peaks to higher angles.

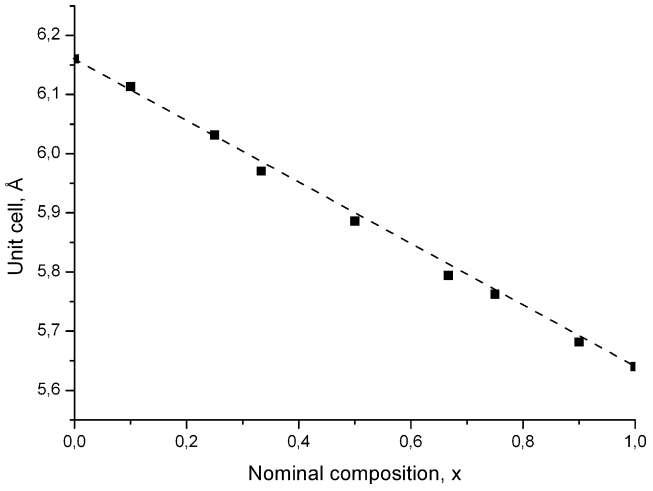

Fig. 2. The refined unit cell parameters for the mixtures, plotted against their nominal composition. The black line represents the linear interpolation (Vegard's law).

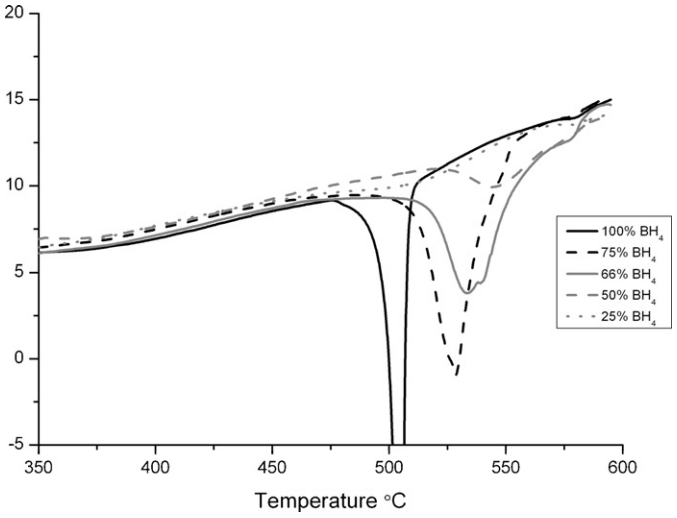

Fig. 3. DSC measurements of different compositions, with a heating rate of 2 °C/min.

This indicates that a small portion of NaCl is dissolved into $NaBH_4$. The NaCl phase remains unaffected. After 6 h of milling the diffraction peaks are broadened over the whole area between the original peaks for $NaBH_4$ and NaCl, indicating a wide range of compositions. A Bragg peak corresponding to a small amount of largely unreacted NaCl remains visible. After both 12 and 24 h the samples contain a single NaCl-type phase, with Bragg peaks positions approximately intermediate of those for $NaBH_4$ and NaCl. This shows that there is an increasing degree of Cl-substitution in $NaBH_4$ with increasing milling time until a single phase is reached. Moreover, the data show that NaCl dissolves faster into $NaBH_4$ than $NaBH_4$ dissolves into NaCl (Fig. 1a). Results from other mixtures show in a similar way that NaCl dissolves into $NaBH_4$ while almost no $NaBH_4$ dissolves into NaCl. This could be explained by the differences in anion size, since the smaller Cl^- anions (ionic radii 1.80 Å, calculated from the unit cell parameter assuming $r(Na) = 1.02$ Å) are expected to diffuse more easily in the larger $NaBH_4$ lattice than the larger BH_4^- anions (ionic radii 2.06 Å, calculated from the unit cell parameter) can diffuse in the smaller NaCl lattice. The PXD patterns indicate that 12 h of milling is sufficient to reach a single NaCl-type $Na(BH_4)_{1-x}Cl_x$ phase for mixtures containing less than 50% $NaBH_4$, while mixtures containing more than 50% $NaBH_4$ still contain two phases after 12 h.

PXD patterns of the samples milled for 24 h (Fig. 1b) show a single phase for all investigated compositions, thus indicating a full homogeneity range between $NaBH_4$ and NaCl. The Bragg peak positions vary systematically with composition as shown for the 220 reflections in Fig. 1b. Rietveld refinements with the lab- or SR-PXD data were used for unit cell determination for all the $NaBH_4$–NaCl mixtures. The results are presented in Table 1 and the unit cell parameters are plotted as a function of sample composition in Fig. 2.

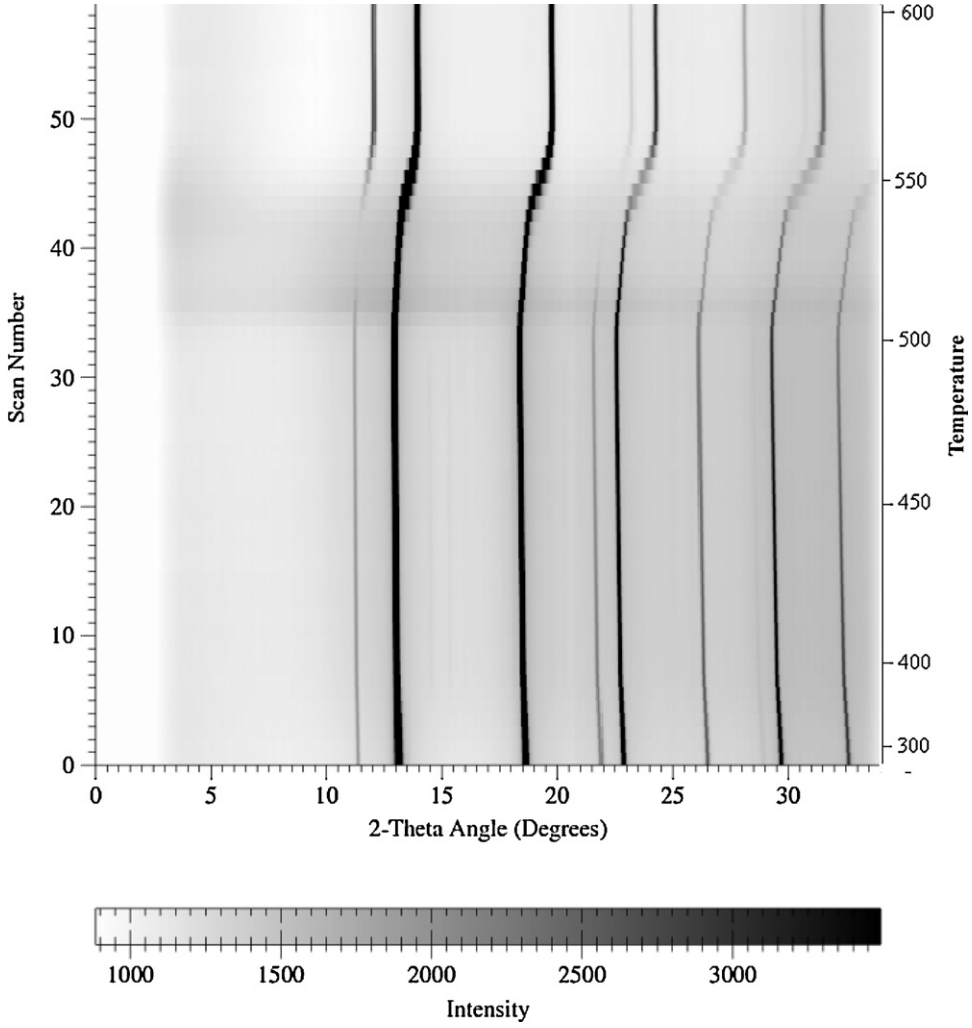

Fig. 4. Image indicating the peak positions from in situ SR-PXD experiment for the sample with 3:1 ratio of $NaBH_4$ and NaCl.

All the unit cell parameters are close to a straight line between the end components, thus indicating Vegard's law behaviour. The compositions estimated from Vegard's law are also listed in Table 1 for comparison and are in agreement with the nominal compositions in the mixtures within 4%.

The DSC measurement of pure $NaBH_4$ only shows one endothermic event corresponding to the melting at 505 °C [10], and no apparent peak corresponding to the decomposition which is reported to occur in the range 534–565 °C [10,13]. However, TPD/RGA shows a strong signal for desorption of hydrogen gas around the melting temperature. The RGA signal for diborane is 4 orders of magnitude lower than that for hydrogen. DSC measurements carried out on the 3:1 and 2:1 samples show no event up to the melting point of $NaBH_4$, and the first endothermic peak is shifted towards higher temperatures, 528 °C and 533 °C, respectively. These peaks are also broadened, thus indicating a gradual change in the samples rather than abrupt melting or decomposition. In mixtures with $NaBH_4$:NaCl ratios $\leq$1 the peaks are so weak and broadened that it is difficult to qualitatively determine the temperatures. However the DSC data show a trend that the first endothermic event is shifted towards higher temperatures with increasing chloride-content (Fig. 3). This means that the chloride substitution stabilizes $NaBH_4$. TPD/RGA measurements confirm that these events are accompanied by hydrogen desorption with only trace amounts of diborane.

The in situ SR-PXD data of the pure $NaBH_4$ sample shows a small shift in the Bragg peak positions towards smaller angles up to 540 °C due to thermal expansion, and then the peaks rapidly disappear between 542 and 550 °C. This is identified as melting. The temperature offset of about 40 °C between the in situ SR-PXD data and the literature-value of 505 °C is ascribed to the fact that the temperature is measured inside the air blower and not on the sample itself. The TPD results confirmed that the melting is followed by decomposition, however, no crystalline decomposition products are observed.

The chloride-containing phases initially show the same small shift in the Bragg peak positions due to thermal expansion upon heating, but then a significant, gradual shift towards larger angles occur around the melting point for pure $NaBH_4$ (Fig. 4). This is interpreted as thermal decomposition of the BH_4^- anions which result in a relative chloride enrichment in the crystalline phase. It is evident from the SR-PXD data that the thermal decomposition of the chloride-containing samples is a gradual process that occurs over a significant temperature range. For the 3:1 sample the shift in 2θ positions towards higher angles takes place in the temperature range 510–566 °C. The positions of the Bragg peaks above these temperatures correspond to the unit cell parameter of pure NaCl [29].

4. Conclusion

The present data show that there is an apparent full homogeneity range between $NaBH_4$ and NaCl. The unit cell parameters of $Na(BH_4)_{1-x}Cl_x$ change in accordance with Vegard's law. The DSC-data indicates a weak stabilization of the substituted phases with increasing chloride-content. The desorption gas is hydrogen with only trace amounts of diborane. The thermal decomposition occurs over a temperature of about 50 °C where the $Na(BH_4)_{1-x}Cl_x$ phase is gradually depleted in BH_4^-. NaCl is the only crystalline final decomposition product after cooling the mixture to ambient temperature and the boron must thus be present in an amorphous state.

Acknowledgements

The Research Council of Norway is acknowledged for financial support through the FRIENERGI project. We acknowledge the skilful assistance from the staff of SNBL at ESRF, Grenoble in France.

References

[1] L. Schlapbach, A. Zuttel, Nature 414 (2001) 353–358.
[2] Y. Nakamori, H.W. Li, K. Kikuchi, M. Aoki, K. Miwa, S. Towata, S. Orimo, J. Alloy Compd. 446 (2007) 296–300.
[3] S.I. Orimo, Y. Nakamori, J.R. Eliseo, A. Zuttel, C.M. Jensen, Chem. Rev. 107 (2007) 4111–4132.
[4] A. Zuttel, A. Borgschulte, S.I. Orimo, Scr. Mater. 56 (2007) 823–828.
[5] U.B. Demirci, P. Miele, C. R. Chim. 12 (2009) 943–950.
[6] Y. Nakamori, K. Miwa, A. Ninomiya, H.W. Li, N. Ohba, S.I. Towata, A. Zuttel, S.I. Orimo, Phys. Rev. B 74 (2006) 9.
[7] K. Miwa, M. Aoki, T. Noritake, N. Ohba, Y. Nakamori, S. Towata, A. Zuttel, S. Orimo, Phys. Rev. B 74 (2006).
[8] K. Chlopek, C. Frommen, A. Leon, O. Zabara, M. Fichtner, J. Mater. Chem. 17 (2007) 3496–3503.
[9] M.D. Riktor, M.H. Sorby, K. Chlopek, M. Fichtner, F. Buchter, A. Zuettel, B.C. Hauback, J. Mater. Chem. 17 (2007) 4939–4942.
[10] Z.K. Sterlyadkina, O.N. Kryukova, V.I. Mikheeva, Russ. J. Inorg. Chem. 10 (1965) 316–318.
[11] R.L. Davis, C.H.L. Kennard, J. Solid State Chem. 59 (1985) 393–396.
[12] J. Urgnani, F.J. Torres, M. Palumbo, M. Baricco, Int. J. Hydrogen Energy 33 (2008) 3111–3115.
[13] P. Martelli, R. Caputo, A. Remhof, P. Mauron, A. Borgschulte, A. Zuttel, J. Phys. Chem. C 114 (2010) 7173–7177.
[14] H.W. Brinks, A. Fossdal, B.C. Hauback, J. Phys. Chem. C 112 (2008) 5658–5661.
[15] N. Eigen, U. Bosenberg, J.B. von Colbe, T.R. Jensen, Y. Cerenius, M. Dornheim, T. Klassen, R. Bormann, J. Alloy Compd. 477 (2009) 76–80.
[16] L. Mosegaard, B. Moller, J.E. Jorgensen, Y. Filinchuk, Y. Cerenius, J.C. Hanson, E. Dimasi, F. Besenbacher, T.R. Jensen, J. Phys. Chem. C 112 (2008) 1299–1303.
[17] L.M. Arnbjerg, D.B. Ravnsbaek, Y. Filinchuk, R.T. Vang, Y. Cerenius, F. Besenbacher, J.E. Jorgensen, H.J. Jakobsen, T.R. Jensen, Chem. Mater. 21 (2009) 5772–5782.
[18] M. Matsuo, H. Takamura, H. Maekawa, H.W. Li, S. Orimo, Appl. Phys. Lett. 94 (2009) 3.
[19] H. Maekawa, M. Matsuo, H. Takamura, M. Ando, Y. Noda, T. Karahashi, S.I. Orimo, J. Am. Chem. Soc. 131 (2009) 894–895.
[20] H. Oguchi, M. Matsuo, J.S. Hummelshoj, T. Vegge, J.K. Norskov, T. Sato, Y. Miura, H. Takamura, H. Maekawa, S. Orimo, Appl. Phys. Lett. 94 (2009) 3.
[21] A. Borgschulte, R. Gremaud, S. Kato, N.P. Stadie, A. Remhof, A. Zuttel, M. Matsuo, S.I. Orimo, Appl. Phys. Lett. 97 (2010).
[22] J.Y. Lee, Y.S. Lee, J.Y. Suh, J.H. Shim, Y.W. Cho, J. Alloy Compd. 506 (2010) 721–727.
[23] B.C. Hauback, N. Aliouane, S. Deledda, J.E. Fonneløp, C. Frommen, H. Grove, K. Lieutenant, I. Llamas-Jansa, S. Satori, M.H. Sørby, International Symposium "Metal-Hydrogen Systems. Fundamentals and Applications", Moscow, Russia, 2010, p. 86.
[24] A.C. Larson, R.B. Von Dreele, General Structure Analysis System (GSAS), Los Alamos National Laboratory Report, LAUR 86-748, 1994.
[25] B.H. Toby, J. Appl. Crystallogr. 34 (2001) 210–213.
[26] A.P. Hammersley, FIT2D: An Introduction and Overview, ESRF Internal Report, ESRF97HA02T, 1997.
[27] S.C. Abrahams, J. Kalnajs, J. Chem. Phys. 22 (1954) 434–436.
[28] J.E. Nickels, M.A. Fineman, W.E. Wallace, J. Phys. Colloid Chem. 53 (1949) 625–628.
[29] D.G.M. Powell, G.C. Fletcher, Aust. J. Phys. 18 (1965) 205–217.